Anal. Chem. **2007,** *79,* 3199−3205

Design for Electrospray Ionization-Ion Mobility Spectrometry

T. Khayamian* and M. T. Jafari

Department of Chemistry, Isfahan University of Technology, Isfahan, 84154, Iran

In this study, a new design for electrospray ionization ion mobility spectrometry (ESI-IMS) was developed. This design has two important differences in comparison to the present ESI-IMS systems. First, a few centimeters of the cell comprising the electrospray needle was located outside of the oven used for heating the IMS cell. This modification prevents prespray solvent evaporation problems such as needle clogging and disturbance of the electrospray process. Second, in addition to the drift gas, a counterflow of a heated gas (desolvation gas) was used between the counter electrode and the ion gate to speed up the desolvation process (Hill, H. H., Jr. *Anal. Chem.* 1998, *70*, 4929−4938). This modification increased the solvent evaporation and resulted in decreasing the drift time, increasing the peak intensity and increasing the resolving power (R_P) or enhancing the resolution for separation of two adjacent ion peaks. In this work, the ion mobility spectra of different compounds including ethion, malathion, metalaxyl, fenamifos, methylamine, triethylamine, tributhylamine, codeine, and morphine were obtained to confirm enhancing of the resolving power of the ion peaks by using the desolvation gas. Furthermore, the method has also been applied to obtain the figures of merit for ethion as a test compound. The linear dynamic range for ethion was in the range 50−1000 μg/L with a limit of quantification of the 50 μg/L.

1. INTRODUCTION

Ion mobility spectrometry (IMS) has been developed as a powerful technique for qualitative and quantitative analysis of the compounds such as illicit drugs,[1,2] explosives,[3,4] and chemical warfare agents.[5,6] The major advantages of this technique are the low detection limit, fast response, simplicity, and portability.[7] The IMS is commonly used for the trace gas analysis. In those methods, the analyte is introduced as a vapor and it is then ionized by different ionization sources such as radioactive sources,[8,9] photodischarge lamps,[10,11] lasers,[12,13] surface ionization sources,[14] and corona discharge.[15−18] In addition, it is possible to introduce liquid samples directly into the IMS using electrospray.[19,20] The electrospray not only ionizes the analyte but also converts the analyte from the liquid phase to the gas phase.

Electrospray ionization was initially employed by Chapman in 1937 to study the gas-phase mobility of several charged carrying liquids in an Erikson mobility tube.[21] Several decades later, based on this idea, the electrospray was introduced as an ionization source for ion mobility spectrometry by Gieniec et al. in 1972.[22] Although the authors reported the spectra of lysozyme in their work, the peaks were very broad due to inefficient solvent evaporation.[23] Later, attempts by Dole et al.[24] to take ion mobility spectra of electrosprayed polystyrene oligomers were unsuccessful, also due to excess solvent ions, which were adsorbed to the surface of the macroion aggregates. Smith et al.[25] also found that it was difficult to separate electrosprayed proteins by IMS due to inefficient desolvation of the electrosprayed droplets. Therefore, the problems associated with ESI-IMS appeared too difficult for

* Corresponding author. Tel.: +98-311-391-2351. Fax: +98-311-391-2350. E-mail: taghi@cc.iut.ac.ir.

(1) Lawrence, A. H. *Anal. Chem.* **1986**, *58*, 1269−1272.
(2) Khayamian, T.; Tabrizchi, M.; Jafari, M. T. *Talanta* **2006**, *69*, 795−799.
(3) Ewing, R. G.; Atkinson, D. A.; Eiceman, G. A.; Ewing, G. J. *Talanta* **2001**, *54*, 515−529.
(4) Khayamian, T.; Tabrizchi, M.; Jafari, M. T. *Talanta* **2003**, *59*, 327−333.
(5) Tuovinen, K.; Paakkanen, H.; Hanninen, O. *Anal. Chim. Acta.* **2001**, *440*, 151−159.
(6) Steiner, W. E.; Clowers, B. H.; Matz, L. M.; Siems, W. F.; Hill, H. H., Jr. *Anal. Chem.* **2002**, *74*, 4343−4352.
(7) Eiceman, G. A.; Karpas, Z. *Ion Mobility Spectrometry*, 2nd ed.; CRC Press: Boca Raton, FL, 2005.
(8) Karasek, F. W. *Res. Dev.* **1970**, *21*, 34−37.
(9) Paakanen, H. *Int. J. Ion Mobility Spectrom.* **2001**, *4*, 136−139.
(10) Baim, M. A.; Eatherton, R. L.; Hill, H. H., Jr. *Anal. Chem.* **1983**, *55*, 1761−1766.
(11) Leasure, C. S.; Fleischer, M. E.; Anderson, G. K.; Eiceman, G. A. *Anal. Chem.* **1986**, *58*, 2142−2147.
(12) Young, D.; Douglas, K. M.; Eiceman, G. A.; Lake, D. A.; Johnston, M. V. *Anal. Chim. Acta.* **2002**, *453*, 231−243.
(13) Gormally, J.; Phillips, J. *Int. J. Mass Spectrom. Ion Processes* **1991**, *107*, 441−451.
(14) Wu, C.; Hill, H. H.; Rasulev, U. K.; Nazarov, E. G. *Anal. Chem.* **1999**, *71*, 273−278.
(15) Tabrizchi, M.; Khayamian, T.; Taj, N. *Rev. Sci. Instrum.* **2000**, *7*, 2321−2328.
(16) Bell, A. J.; Ross, S. K. *Int. J. Ion Mobility Spectrom.* **2002**, *5*, 95−99.
(17) Tabrizchi, M.; Abedi, A. *Int. J. Mass Spectrom.* **2002**, *218*, 75−85.
(18) Borsdorf, H.; Rammler, A.; Schulze, D.; Boadu, K. O.; Feist, B.; Weiss, H. *Anal. Chim. Acta* **2001**, *440*, 63−70.
(19) Shumate, C. *Trends Anal. Chem.* **1994**, *13*, 104−109.
(20) Wittmer, D.; Chen, Y. H.; Luckenbill, B. K.; Hill, H. H., Jr. *Anal. Chem.* **1994**, *66*, 2348−2355.
(21) Chapman, S. *Phys. Rev.* **1937**, *52*, 184−190.
(22) Gieniec, M. L.; Cox, J., Jr.; Teer, D.; Dole, M. *Proceedings of the 20th Annual Conference on Mass Spectrometry and Allied Topics*, Dallas, TX, June 4−9, 1972.
(23) Wu, C.; Siems, W. F.; Asbury, G. R.; Hill, H. H., Jr. *Anal. Chem.* **1998**, *70*, 4929−4938.
(24) Dole, M.; Gupta, C. V.; Mack, L. L.; Nakamae, K. *Polym. Prepr.* (*Am. Chem. Soc., Div. Polym. Chem.*). **1977**, *18*, 188−193.
(25) Smith, R. D.; Loo, J. A.; Ogorzalek, R. R.; Busman, M. *Mass Spectrom. Rev.* **1991**, *10*, 359−451.

10.1021/ac062381q CCC: $37.00
Published on Web 03/17/2007

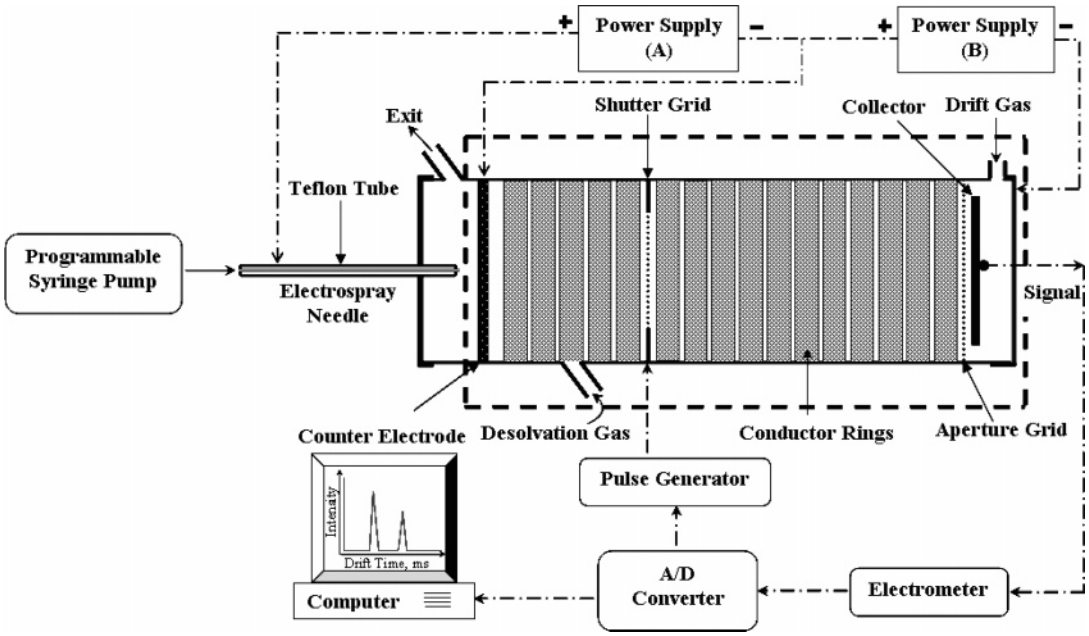

Figure 1. Side view schematic diagram of the electrospray ionization-ion mobility spectrometer apparatus. The IMS cell was divided into a drift region (11 cm), a desovation region (4 cm), and an electrospray region (3 cm), which the electrospray needle was located outside of the heating oven (dashed lines). In addition to the drift gas, the desolvation gas was introduced into the dsolvation region to speed up the desovation process.

practical application, and it was concluded that the electrospray would only be useful as an ionization source for mass spectrometry (MS).[26] For this reason, the majority of electrospray researches shifted to MS in the late 1980s and 1990s.[27,28] Then Shumate and Hill[29] used the heated and unidirectional flow of nitrogen as the drift gas for increasing of the desolvation efficiency in ESI-IMS; however, the evaporation of the solvent from the ion droplets in the drift region caused band broadening of the ion peak.[19,29] Furthermore, the difficulty with this initial counterflow ESI-IMS design was that the heated drift gas raised the temperature of the electreospray needle sufficiently to cause prespray solvent evaporation problem.[28] In 1994, Wittmer et al.[20] developed a water-cooled electrospray ionization source included rapid desolvation of sprayed droplets and prevention of solute precipitation in the spray needle. After this, Hill and co-workers used a gas-cooled system in addition to water-cooled jacket, to prevent solvent evaporation inside the needle.[27,28,30] This cooled electrospray system has been used for separation of multiply charged states of cytochrom *c* and ubiquitin,[23] chemical warfare degradation products,[31] isomeric peptides,[32] and detection of illicit drugs.[33]

In this work, a new IMS cell was designed, by locating the electrospray needle outside of the heating oven and applying a new gas flow (desolvation gas), to speed up the desolvation process and to prevent analyte deposition at the needle tip. The ion mobility spectra were obtained for compounds from different categories such as pesticides, narcotics and amines. The results demonstrated enhancement of the resolving power of the compounds. In addition, the quantitative ability of the method was confirmed by analyzing ethion as a test compound.

2. EXPERIMENTAL SECTION

2.1. Instrumentation. The electrospray ionization ion mobility spectrometer used in this study was constructed in-house at Isfahan University of Technology. The schematic diagram of the apparatus is shown in Figure 1. The IMS cell was made of a glass tube, 4 cm inner diameter and 19 cm long, on which 16 stainless steel guard rings, located 1 mm from each other are mounted. The guard rings are electrically connected by a series of megaohm resistors to form a uniform electric field. The IMS cell length was divided into three regions, the electrospray region (3 cm), the desolvation region (4 cm in length), and the drift region (11 cm). The electrospray region was separated from the desolvation region by the counter electrode and the desolvation region was separated from the drift region by a Bradbury−Nielsen ion gate. The gate can be "closed" by applying 85 V across the wires, and when "open," the gate was referenced to the drift field voltage. An oven with a sufficient volume was constructed to warm up the cell. In this design a part of the cell, comprising the electrospray needle was located outside of the oven. Therefore, it is possible to observe the needle tip by illuminating it by a small diode laser. This modification allows the operator to observe the needle tip and to optimize the experimental conditions for producing a plume formation and a stable electrospray. A stable electrospray has a cone with an electrospray plume. The drift tube temperature was set at 130 °C for all the experiments. Two separate high voltage supplies (A and B) were used so that the needle voltage and the drift voltage could be set independently. The needle and the drift power supplies were the 10 kV isolated and 10 kV non-isolated

(26) Gieniec, J.; Mack, L. L.; Nakamae, K.; Gupta, C.; Kumar, V.; Dole, M. *Biomed. Mass Spectrom.* **1984**, *11*, 259−268.
(27) Asbury, G. R.; Hill, H. H., Jr. *Int. J. Ion Mobility Spectrom.* **1999**, *2*, 1−8.
(28) Chen, Y. H.; Hill, H. H., Jr.; Wittmer, D. P. *Int. J. Mass Spectrom. Ion Proc.* **1996**, *154*, 1−13.
(29) Shumate, C. B.; Hill, H. H., Jr. *Anal. Chem.* **1989**, *61*, 601−606.
(30) Lee, D. S.; Wu, C.; Hill, H. H., Jr. *J. Chromatogr., A* **1998**, *822*, 1−9.
(31) Asbury, G. R.; Wu, C.; Siems, W. F.; Hill, H. H., Jr. *Anal. Chim. Acta* **2000**, *404*, 273−283.
(32) Wu, C.; Siems, W. F.; Klasmeier, J.; Hill, H. H., Jr. *Anal. Chem.* **2000**, *72*, 391−395.
(33) Wu, C.; Siems, W. F.; Hill, H. H., Jr. *Anal. Chem.* **2000**, *72*, 396−403.

Table 1. Typical Experimental Parameters

operating parameters	setting
needle voltage	11.2 kV
counter electrode voltage	9.0 kV
drift region length	11 cm
desolvation region length	4 cm
drift field	600 V/cm
desolvation field	600 V/cm
liquid flow rate	10 μL/min
drift gas flow (N_2)	500 mL/min
desolvation gas flow (N_2)	900 mL/min
drift tube temperature	130 °C
drift gas temperature	100 °C
desolvation gas temperature	100 °C
shutter grid Pulse	0.3 ms

power supplies, respectively. A commercially available 25-gauge polished needle (P/N 80726, Hamilton) with 0.006 in. i.d. and 0.020 in. o.d. was used as the electrospray needle. The length of the needle was approximately 5.5 cm, and the end of it was pushed and tightened through a ferrule in the steel nut for connection to the syringe. The steel nut, which was connected to the power supply, was covered with a Teflon tube to prevent sparking between the needle and the syringe pump. The needle was also insulated with a Teflon tube, except the half millimeter of its tip. This is necessary to prevent corona discharge.[20,28] The counter electrode was a stainless steel ring with 5 mm width and located inside the cell, at a 4 cm distance from the shutter grid. A dual-piston syringe pump (Kent Scientific Co., U.S.A) was employed for liquid delivery through the needle. The electrospray flow rate was maintained at 10 μL min^{-1} for all the experiments and the electrospray was developed by applying a 2.2 kV potential between the needle and the counter electrode. Pure nitrogen was employed as the drift and the desolvation gas with flow rates of 500 and 900 mL min^{-1}, respectively. The gas was filtered with a 13× molecular sieves (Fluka) trap before it was entered into the IMS cell in order to remove water vapor or other contamination. The drift and desolvation gases were preheated by means of two hot steel cylinders (~4 L volume) prior to entering into the cell. Each cylinder was equipped with a heating element for maintaining of the temperature of the gas at 100 °C. According to the Figure 1 the desolvation gas was introduced into the desolvation region through a glass tube joint, an angle of 45° with respect to the cell. Therefore, the flow direction of the desolvation gas was the same as the drift gas and in the opposite to the direction of ion migration. The optimized experimental conditions for obtaining the ion mobility spectra of the compounds are listed in Table 1. It should be noted that all the IMS spectra shown in this work were the average of 50 spectra.

2.2. Chemicals and Solutions. Methanol as the solvent was analytical grade and purchased from Merck. The pesticides including ethion, malathion, fenamifos, and metalaxyl were prepared from Accustandard, Inc. Stock standard solution of 100 μg/mL ethion was prepared in methanol. Working solutions (0.02−20 μg/mL) were prepared by successive dilution of the stock solution. All the amines used in this work were purchased from Merck. Morphine sulfate and codeine phosphate were prepared from Temad Co. (Tehran).

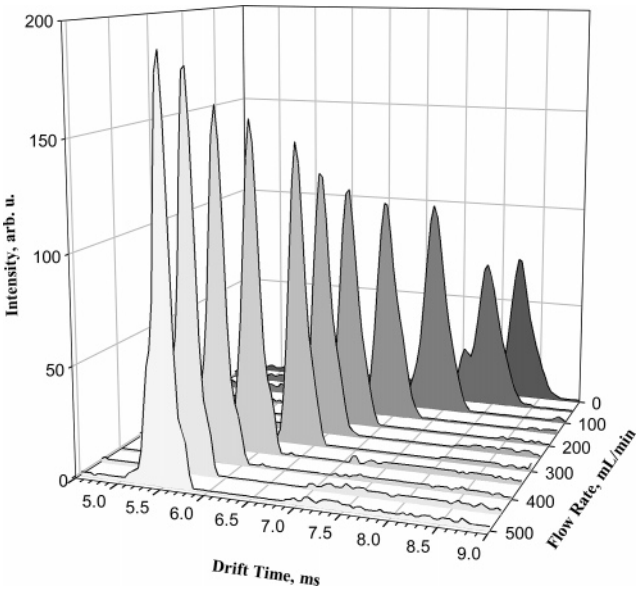

Figure 2. The 3D plot of the ion mobility spectra of the solvent at different flow rates of the drift gas, when the flow rate was increased from 0 to 500 mL/min. The drift time of the solvent major peak reduced from the 8.20 to 5.68 ms, where the intensity of the solvent major peak increased from the 70 to the 180 arbitrary unit.

3. RESULTS AND DISCUSSION

In this new design, the electrospray needle was located outside the heating oven and therefore, it was not necessary to cool the needle to prevent solvent evaporation at the needle tip. In the other words, the electrospray source is not incorporated as an integrated part of the drift tube in a closed oven. This modification prevents prespray solvent evaporation problems such as needle clogging and disturbances of the electrospray process.

3.1. Desolvation Process. In order to investigate the capability of the desolvation gas for the solvent evaporation, two series of experiments were conducted with and without using of the desolvation gas. In these experiments ion mobility spectra of methanol as the solvent were recorded at different flow rates of the drift gas and desolvation gas. The first series of the solvent spectra were obtained at different drift gas flow rates without using the desolvation gas. The results, which are shown in Figure 2, demonstrate that with increasing the drift gas flow rate, the drift time of the solvent peak decreases. This would be expected, because at higher flow rates, desolvation of the ions occurs more efficiently and consequently faster ions are formed. This process was continued up to a flow rate of 500 mL/min at which poorly resolved peak were obtained at 5.68 (major) and 5.48 ms. However, at flow rate higher than 500 mL/min, the mobility of the solvent peaks are decreased and the drift time begins to increase. This could be due to increasing pressure inside the cell at high flow rates of the drift gas.

The second series of ion mobility spectra of the solvent were recorded at different flow rates of the desolvation gas and a constant flow rate of the drift gas (500 mL/min). These spectra are shown in Figure 3. According to this figure, increasing the desolvation gas flow rate decreases the drift time of the solvent peaks because of the easier solvent evaporation. Figure 3 shows that increasing flow rates of the desolvation gas (0−900 mL/min) larger ion currents are observed, and more importantly, the

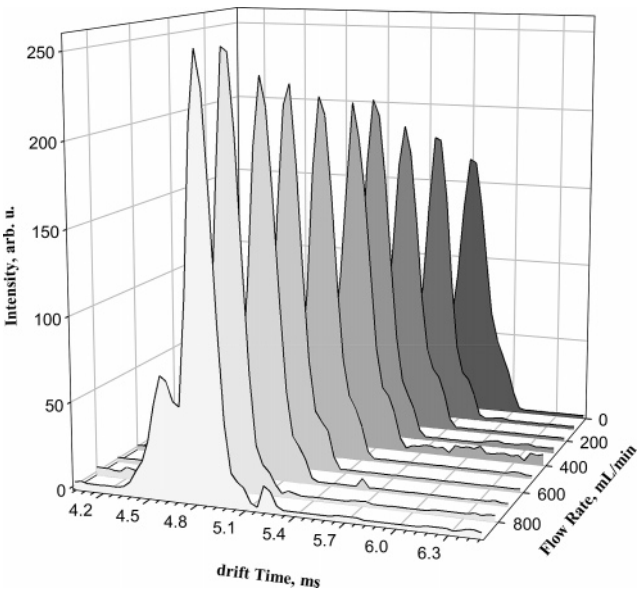

Figure 3. The 3D plot of the ion mobility spectra of the solvent in different flow rates of the desolvation gas and a constant flow rate of the drift gas (500 mL/min), when the flow rate of the desolvation gas was increased from 0 to 900 mL/min. The drift time of the solvent major peak reduced from 5.68 to 4.88 ms, where the intensity of the solvent major peak increased from the 170 to the 250 arbitrary unit.

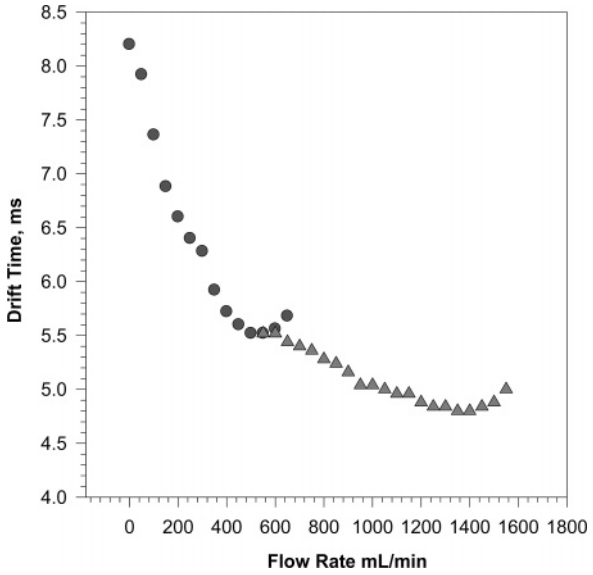

Figure 4. Drift time of the solvent major ion peak versus flow rate of the drift and desolvation gases, (blue circle) Drift gas in absence of desolvation gas and (red triangle) desolvation gas at a constant flow of the drift gas (500 mL/min). Comparison of these two plots shows that the desolvation process is speeded up by introducing the desolvation gas as the same as the drift gas, but with a smaller slope.

ion peaks became narrower, resulting in the higher resolution. The solvent peaks are resolved well at desolvation gas flow of 900 mL/min; presumably, the number of clustered solvent ions is decreased. In order to show the effect of the drift gas and desolvation gas on the desolvation process, the drift time of the major solvent ion peak was plotted versus the sum of the flow rates of both gases. The results are shown in Figure 4. It should be noted that when the desolvation gas flow rate is increased, the drift time of the solvent major peak is decreased, however, with a smaller slope than that of the drift gas. The optimum

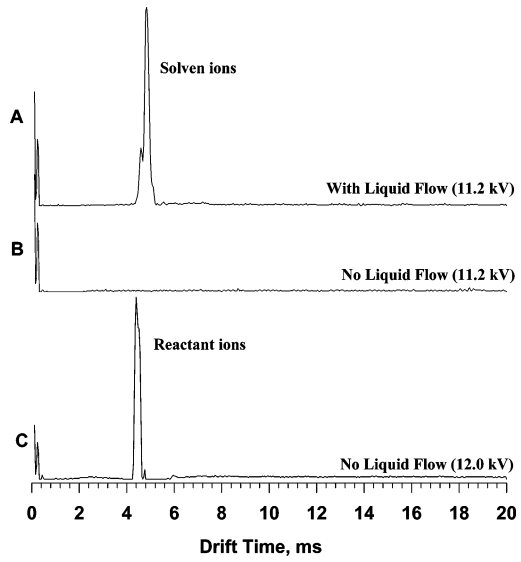

Figure 5. The ion mobility spectra of the background with (A) and without (B) solvent delivery through the electrospray needle (at the needle voltage of 11.20 kV). (C) The ion mobility spectrum of the background using corona discharge (3.00 kV between the electrospray needle and counter electrode). This figure illustrates the condition of true electrospray obtained at operating conditions (Table 1).

desolvation gas and drift gas flow rates were obtained at 500 and 900 mL/min, respectively.

In conclusion, the results of these figures can be explained by considering the electrospray process and the influences of the drift and desolvation gases on this process. In electrospray process, ion solvent clusters with different numbers of solvent molecules are produced. The drift and desolvation gases evaporate some solvent molecules from these clusters to produce ion clusters with lower and more uniform molecular weight, resulting ions with a higher mobility. These gases also enhance intensity, because ion clusters are converted to clusters with the lower numbers of solvent molecules, producing a narrower peak and consequently a higher intensity.

3.2. Electrospray Ionization. The ion mobility spectra of the background, with and without solvent flow through the needle are shown in Figure 5. In addition, the ion mobility spectrum of the background using the corona discharge, appeared at a higher voltage, is also shown in Figure 5. In this work, when methanol solvent was delivered through the needle, no current could be measured when the difference between the electrospray needle and counter electrode was below 1.80 kV—that is, when the needle potential was adjusted to about positive 10.80 kV and a counter electrode to a positive 9.00 kV. Beyond this voltage, the unstable plume of electrospray appeared. However, when the needle voltage was increased to 11.20 kV (spray voltage of 2.20 kV), a stable plume was observed, characterized by the appearance of the "Taylor cone" at the needle tip. In this case, a background spectrum of solvent was obtained which is shown in Figure 5A. The ion mobility spectrum of methanol consisted of two solvent ion peaks and is the same as that reported by Chen et al.[34] When the voltage was increased beyond that of the Taylor cone

(34) Chen, Y. H.; Siems, W. F.; Hill, H. H., Jr. *Anal. Chim. Acta.* **1996**, *334*, 75−84.

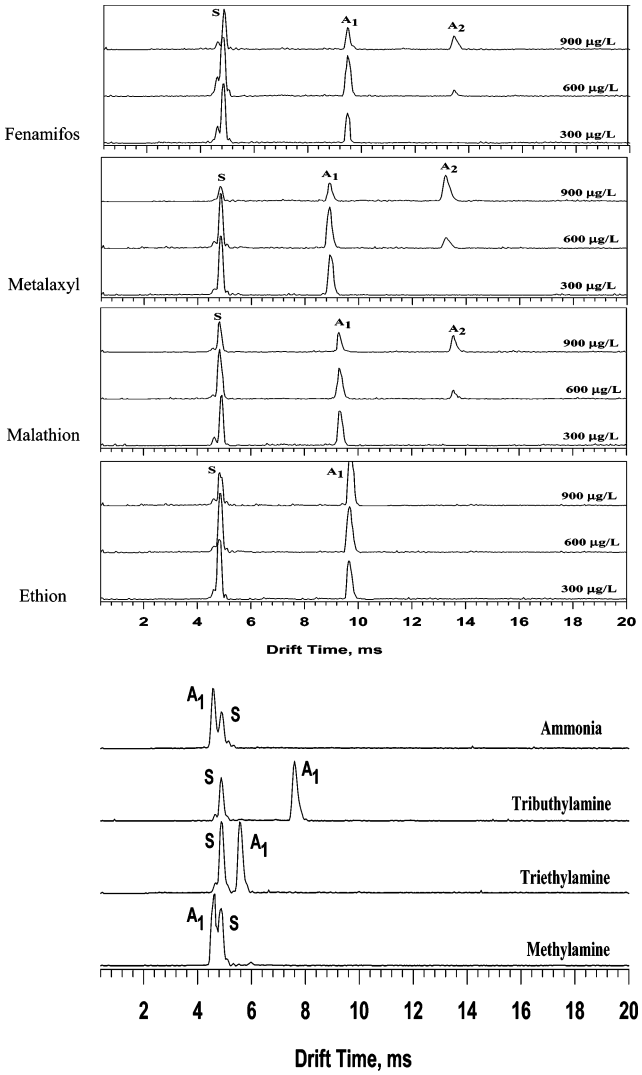

Figure 6. Top: ion mobility spectra of pesticides at different concentrations. Bottom: ion mobility spectra of amines compounds, (S) solvent peak, (A_1) analyte protonated monomer, and (A_2) the dimer ion of the compounds. All of the spectra recorded at the optimized condition (Table 1) and averaged of 50 spectra. The scale of y-axes (intensity) is the same for each spectrum.

Table 2. The Resolving Power for Ion Peaks of Several Compounds

	resolving power, R_P	
compound	no desolvation flow	with desolvation flow (900 mL/min)
ethion	32.5 ± 0.7	41.0 ± 0.6
malathion	32.5 ± 0.3	40.7 ± 0.9
metalaxyl	50.7 ± 0.8	59.7 ± 0.8
tributhylamine	27.3 ± 0.4	34.5 ± 0.6

formation, this single cone was disappeared and the several smaller jets could be observed and finally the unstable plume of electrospray would be appeared. Figure 5B shows the ESI-IMS background at the needle voltage of 11.20 kV when the solvent delivery was stopped. In this work, the spray needle was insulated with Teflon tubing to eliminate the corona discharge.[20,28] According to Figure 5B, no current could be measured, indicating that corona discharge cannot be formed under these circumstances.

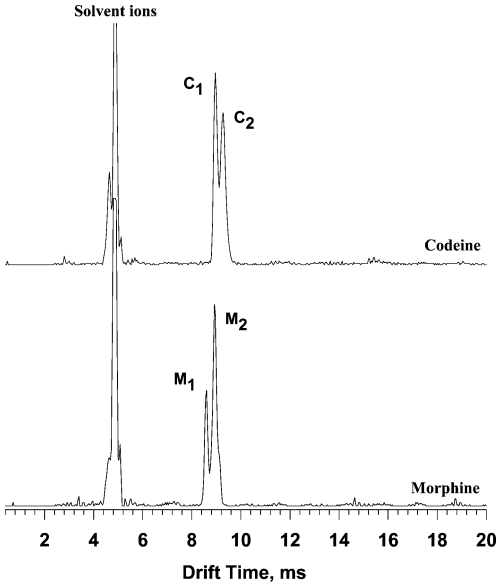

Figure 7. The ion mobility spectra of morphine and codeine, showing two resolved ion peaks for each compound.

However, when the needle voltage was increased to 11.80 kV, the background spectrum included reactant ions which originated from the unstable corona discharge phenomena. At a higher voltage, 12.00 kV, a stable corona discharge appeared and its background spectrum is shown in Figure 5C. It has been shown by MS that the ions produced with electrospray and corona discharge could be different.[28,29]

3.3. Ion Mobility Spectra. The ion mobility spectra of three classes of compounds were obtained at the optimized conditions. Figure 6 shows the ion mobility spectra of ethion, malathion, fenamifos, and metalaxyl as the pesticides group, with different concentrations. This figure shows that the spectra were changed for fenamifos, metalaxyl, and malathion because of formation of the dimer ion for these compounds at higher concentrations. In addition, the ion mobility spectra of ammonia, methylamine, triethylamine, and tributhylamine are also shown in this figure. The reduced mobility values of the produced ions for all the compounds studied in this work are listed in Table 2. In addition in Table 2, the reduced mobility values of these compounds reported in the literatures using ^{63}Ni and electroapray are also tabulated. As shown in Table 2, most K_o values reported in this study are in good agreement with those obtained by other ESI-IMS reports, but they are different from K_o values reported using ^{63}Ni. However, they show similar trends. Exceptions in this table are the reduced mobility values for ammonia and methylamine, which appeared in the region of the background solvent peaks. Such exceptions have also been reported by Wittmer et al.[20] They have explained that lower K_o values for low molecular weight compounds such as ammonia and methylamine are related to inadequate desolvation of these ions. Kebarle and Tang[35] have also reported the high solvation energy for small ions such as ammonium. Therefore, inadequate desolvation of ammonium and methylamine can be attributed to the high salvation energies of these ions. The greater K_o values observed in the present work for ammonia and methylamine with respect to the results of

(35) Kebarle, P.; Tang, L. *Anal. Chem.* **1993**, *65*, 972−986.

Table 3. Reduced Mobility Values (K_o) and Literature K_o Values for Several Compounds Employed in This Study

compound	class	drift time (ms)	K_o ($cm^2\ V^{-1}\ s^{-1}$)	lit. K_o ($cm^2\ V^{-1}\ s^{-1}$) (ESI)	lit. K_o ($cm^2\ V^{-1}\ s^{-1}$) (^{63}Ni)[a]
Ammonia	Industerial	4.56	2.25 ± 0.05	1.86 (20)	3.02 (20)
Methylamine	Industerial	4.64	2.21 ± 0.05	1.75 (20)	2.65 (20)
Triethylamine	Industerial	5.56	1.84 ± 0.04	1.85 (20)	1.95 (20)
Tributhylamine	Industerial	7.60	1.35 ± 0.04	1.36 (20)	1.38 (20)
Ethion	Pesticide	9.68	1.06 ± 0.01		1.20 (39)
Malathion	Pesticide	9.24	1.11 ± 0.02		1.30 (39)
		13.52[b]	0.76 ± 0.01		
Metalaxyl	Pesticide	8.88	1.15 ± 0.03		
		13.20[b]	0.77 ± 0.02		
Fenamifos	Pesticide	9.48	1.08 ± 0.02		
		13.48[b]	0.76 ± 0.01		
Morphine	Narcotic	8.60	1.19 ± 0.04	1.14 (36)	1.26 (1)
		8.92	1.15 ± 0.04	1.11 (36)	1.22 (1)
Codeine	Narcotic	8.96	1.14 ± 0.03	1.10 (36)	1.21 (1)
		9.28	1.10 ± 0.02	1.07 (36)	1.18 (1)

[a] The reference values were obtained with air as the drift gas. Parentheses contain the reference number. [b] The peack is might be due to the dimer ion formation.

reference 20 can might be due to high desolvation efficiency of this new design.

The ion mobility spectra of morphine and codeine are shown in Figure 7. According to this figure, two separately peaks, C_1 and C_2, with K_o of 1.14 and 1.10 $cm^2\ V^{-1}\ s^{-1}$, respectively, are observed for codeine spectrum. The morphine spectrum also shows two separately peaks, M_1 and M_2 with reduced mobility (K_o) values of 1.19 and 1.15 $cm^2\ V^{-1}\ s^{-1}$, respectively. Matz and Hill[36] have reported reduced mobility of 1.10 and 1.07 $cm^2\ V^{-1}\ s^{-1}$ for codeine assigned $(M-H_2O)^+$ and $(MH)^+$, respectively using ESI-IMS/MS. They have also reported the same type of ions with reduced mobility of 1.14 and 1.11 $cm^2\ V^{-1}\ s^{-1}$ for morphine. From comparison of the reduced mobility values of this work and the reported values for these compounds,[36] it might be concluded that the first (M_1 and C_1) and the second (M_2 and C_2) ion peaks are $(M-H_2O)^+$ and $(MH)^+$, respectively. However, it should be emphasized that the coupling of IMS to a mass spectrometer is needed for the complete characterization of the chemical formula of the product ions.

3.4. Resolving Power. In order to investigate the performance of the instrument, resolving power values for different compounds were measured. The resolving power (R_P) was calculated based on the single-peak-based quotient:[23]

$$R_P = t_d/w_{1/2} \quad (1)$$

where, t_d is the drift time of the ion peak and $w_{1/2}$ is the ion pulse duration at half of the maximal intensity, in milliseconds. The measured resolving power of the ion peaks for four compounds are shown in Table 3. According to these results, the resolving power of the compounds was enhanced 18−26% when the desolvation gas was introduced into the IMS cell. The desolvation gas speeds up the solvent evaporation process in the desolvation region, before the ions are injected into the drift region. Solvent evaporation in the drift region causes band broadening of the ion peaks[19,29] but solvent evaporation in the desolvation region reduce peak width and enhance the resolving power. A practical consequence of increasing of the resolving power is the ability to separate closely spaced peaks. In this regard, the separation efficiency was calculated in terms of peak-to-peak resolution,[37] R_{pp}, using eq 2:

$$R_{pp} = \left(\frac{2\Delta t_d}{w_{b1} + w_{b2}}\right) \quad (2)$$

where Δt_d is difference between the drift times of the two adjacent peaks and the w_{b1} and w_{b2}, are their peak width. For example,

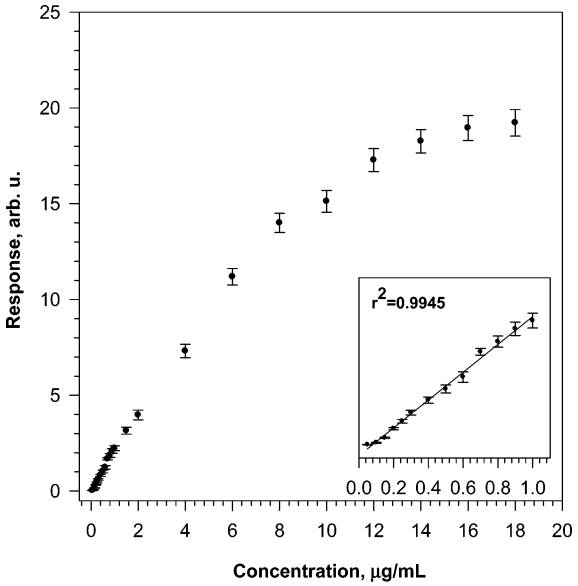

Figure 8. The response of ESI-IMS versus the concentration of ethion as a test compound. The working range is from about 0.05 to 16.00 µg/mL. The plot shown as onset of this graph indicates the linear section of the calibration curve for ethion in range of 0.05−1.00 µg/mL or about 2 orders of magnitude. The error bars for the data points are shown.

(36) Matz, L. M.; Hill, H. H., Jr. *Anal. Chem.* **2001**, *73*, 1664−1669.

(37) Dion, H. M.; Ackerman, L. K.; Hill, H. H., Jr. *Talanta* **2002**, *57*, 1161−1171.

Table 4. Analytical Parameters for Ethion Determination Using ESI-IMS

parameter	value
linear dynamic range (μg/L)	50−1000
working range (μg/mL)	0.05−16
correlation coefficient, R^2	0.994
detection limit (μg/L)	19
limit of quantification (μg/L)	50
relative standard deviation, RSD ($n = 3$, 100 μg/L)	10.5

when the desolvation gas was introduced into the cell, the resolutions of ion peaks were enhanced from 1.67 to 2.00 for methanol and from 0.77 to 1.00 for codeine.

3.4. Figures of Merit. The extensive quantitative investigation has not been attempted using ESI-IMS, although the quantitative surveys of rather limited numbers of the compounds have been reported.[31,33,38] In this work, the ability of the instrument was examined by analysis of ethion as a test compound. In this work, the area of ion peak was considered as the response. Figure 8 shows the working range for ethion in methanol solutions. The working range is plotted in the range 0.05−16 μg/mL. The plot shown as onset of this figure shows the linear section of the calibration curve. This graph shows a linear response for ethion in the range of 50−1000 μg/L, with a correlation coefficient of 0.9945. This is a typical linear dynamic range for ESI sources and for most of the IMS instruments.[31] The quantification limit of 50 ng/mL was determined for ethion. This limit of quantification can be compared well with the range of 10−1340 ng/mL reported by Asbury et al.[31] or with the results obtained using ^{63}Ni−IMS, for various organophosphorus compounds.[39] The analytical parameters of proposed ESI-IMS method for the determination of ethion are given in Table 4. The results demonstrated a strong potential of the method and the instrument as an analytical tool for the detection of various compounds in liquid samples.

(38) Matz, L. M.; Hill, H. H., Jr. *Anal. Chem.* **2002**, *74*, 420−427.
(39) Jafari, M. T. *Talanta* **2006**, *69*, 1054−1058.

4. CONCLUSIONS

A new IMS cell was designed and constructed. In this design, the electrospray needle was located outside of the cell oven. In addition, a desolvation gas flowing through the cell was also added. The consequences of these changes were to prevent needle clogging, increase the peak intensity and to improve the resolving power of the apparatus. Furthermore, the analytical parameters for ethion demonstrated the excellent performance of the method for quantitative analysis.

ACKNOWLEDGMENT

We express our appreciation to the Research Council of Isfahan University of Technology for financial support of this work. Valuable discussions with Dr. M. Tabrizchi and Dr. M.K. Amini are specially acknowledged.

Received for review December 17, 2006. Accepted February 8, 2007.

AC062381Q